DENTAL MATERIALS XXX (2021) XXX.E1–XXX.E11

Available online at www.sciencedirect.com

ScienceDirect

journal homepage: www.intl.elsevierhealth.com/journals/dema

Physicochemical and mechanical characterization of a fiber-reinforced composite used as frameworks of implant-supported prostheses

Edmara T.P. Bergamo[a,*], *Tiago M.C. Bastos*[b], *Adolfo C.O. Lopes*[a], *Everardo N.S. de Araujo Júnior*[a], *Paulo G. Coelho*[c], *Ernesto B. Benalcazar Jalkh*[a,c], *Abbas Zahoui*[a], *Estevam A. Bonfante*[a]

[a] *Department of Prosthodontics and Periodontology, University of São Paulo, Bauru School of Dentistry, 9-75, Otávio Pinheiro Brisola, 17012-901, Bauru, SP, Brazil*

[b] *Department of Physics, Technological Institute of Aeronautics, 50 Marechal Eduardo Gomes, 12228-900, São José dos Campos, SP, Brazil*

[c] *Department of Biomaterials and Biomimetics, Hansjorg Wyss Department of Plastic Surgery, Mechanical and Aerospace Engineering, New York University, 345 24th Street, 10010, New York City, NY, USA*

ARTICLE INFO

Article history:
Received 14 May 2020
Received in revised form
31 December 2020
Accepted 29 March 2021
Available online xxx

Keywords:
Dental materials
Dental prosthesis
Dental implants

ABSTRACT

Objectives. To characterize the physicochemical and mechanical properties of a milled fiber-reinforced composite (FRC) for implant-supported fixed dental prostheses (FDPs).

Methods. For FRC characterization, scanning electron microscopy (SEM), energy dispersive spectroscopy (EDS), X-ray diffraction, Fourier-transformed infrared spectrometry, simultaneous thermogravimetric analysis and differential scanning calorimetry were performed. For fatigue testing, 3-unit FRC frameworks were fabricated with conventional (9 mm^2 connector area) and modified designs (12 mm^2 connector area and 2.5 mm-height lingual extension). A hybrid resin composite was veneered onto the frameworks. FDPs were subjected to step-stress accelerated-life fatigue testing until fracture or suspension. Use level probability Weibull curves at 300 N were plotted and the reliability for 100,000 cycles at 300, 600 and 800 N was calculated. Fractographic analysis was performed by stereomicroscope and SEM.

Results. The FRC consisted of an epoxy resin (~25%) matrix reinforced with inorganic particles and glass fibers (~75%). Multi-layer continuous regular-geometry fibers were densely arranged in a parallel and bidirectional fashion in the resin matrix. Fatigue analysis demonstrated high probability of survival (99%) for FDPs at 300 N, irrespective of framework design. Conventional FDPs showed a progressive decrease in the reliability at 600 (84%) and 800 N (19%), whereas modified FDPs reliability significantly reduced only at 800 N (75%). The chief failure modes for FRC FDPs were cohesive fracture of the veneering composite on lower loads and adhesive fracture of the veneering composite at higher loads.

* *Corresponding author.*
E-mail address: edmaratatiely@gmail.com (E.T.P. Bergamo).

https://doi.org/10.1016/j.dental.2021.03.014

Significance. Milled epoxy resin matrix reinforced with glass fibers composite resulted in high probability of survival in the implant-supported prosthesis scenario.

1. Introduction

Advances in oral implantology including new implant designs and surface topography have consolidated implant therapy as a reliable long-term alternative to restore from single missing tooth to complete arch edentulousness, even for immediate implant loading protocols [1–4]. Despite the proven clinical success of osseointegration, implant-supported reconstructions have exhibited biological and mechanical complications, mainly for long-span prostheses, which influences clinical outcomes [5,6]. Irrespective of restorative system, implant-supported prostheses exhibited higher levels of technical complications relative to tooth-supported prostheses [7], for factors including the absence of mechanoreceptors and their peripheral feedback mechanism that differentiate food hardness and texture, as well as periodontal ligament and its inherent resilience to absorb occlusal forces [8–10]. The biomechanical behavior of implant reconstructions has been previously shown to be influenced by the physical-mechanical properties, geometry and three-dimensional position of the prosthetic constituents, thus technological improvements in the bioengineering field has focused on the development/improvement of biomechanically favorable restorative systems to meet the functional and esthetic demands of the oral cavity [8,9,11–16].

Composites are usually referred to systems that combine two or more constituents with different composition and/or morphology, presenting a synergistic benefit of their best properties [17]. From the aerospace and aeronautical fields, fiber-reinforced composites (FRC) have emerged as a promising class of material also to advanced biomedical application due to their high strength and stiffness to weight ratios [14,15,17,18]. Dental FRCs generally consist of inorganic particles and fibers as reinforcing compounds bonded to a polymeric matrix by a coupling agent, ending at a remarkable increase in the consumed fracture energy during crack growth, known as resistance curve (R-curve) behavior inherent to such restorative systems (σ: 540−740 MPa, E: 30 GPa) [13,15,19]. The properties of FRC systems are directly influenced by fiber type, fiber volume fraction within the matrix, fiber architecture and orientation, polymer matrix used, and interfacial adhesion between fiber and matrix [13,20]. FRC-based dental rehabilitations may offer significant clinical advantages in terms of cost effectiveness, chemical adhesion to resin cement, and reparability [13,15,18,20,21]. Moreover, a promising biomechanical performance can be expected for FRC rehabilitations, especially for implant-supported reconstructions, not only due to their high strength but also their low elastic modulus that may increase the material resilience and, consequently, favor chewing forces dampening and stress distribution [8,9,15,16].

The clinical performance of FRC prostheses has shown to be dictated by an appropriate dimension, geometry, and three-dimensional location of the framework, following a structural relationship with occlusal forces distribution [13–15,17]. To obtain the maximum performance out of FRC frameworks, fibers should be parallelly aligned with the maximum principal stress direction [13–17]. Tooth-supported reconstructions have demonstrated high survival rates (94.4% after 5 years in function) for FRC FDPs, with fracture of the veneering composite (9.5%) and infrastructure (3.7%) being the most frequently reported complications [18]. Such unfavorable events can be associated with an insufficient occlusal support provided by the unidirectional fiber alignment as well as the manual fabrication of conventional FRC, which may involve a higher density of defects due to voids formation and compromised fiber/matrix adhesion that has previously shown to decrease the resistance of the material to up to 10% [13,14,18,22].

Therefore, FRC systems for computer-aided design/computer-aided manufacturing (CAD/CAM) use have recently gained attention since discs are industrially fabricated under controlled parameters of temperature and pressure, resulting in reduced defect population and increased structural reliability, as well as fibers alignment can be more precisely arranged in different directions [23–26]. In addition, an anatomic fabrication of tooth- and implant-supported prosthetic constituents can be planned [23–25]. However, the literature is scarce in addressing FRC CAD/CAM systems performance [15]. Hence, the present study aimed to characterize the physicochemical and mechanical properties of a recently developed FRC system for CAD/CAM use (Zantex Discs, Bionfunctional Materials, QF: 061.03), and to evaluate the reliability and failure mode of FDPs with two different framework designs for 3-unit posterior implant-supported prosthesis, under step-stress accelerated life (SSALT) testing. The postulated null hypothesis was that framework design would not affect FRC FDP performance.

2. Materials and methods

2.1. *Fiber-reinforced composite characterization*

A recently developed fiber-reinforced composite (FRC) (Zantex, Biofunctional Materials, Boca Raton, FL, USA) for CAD/CAM use was characterized in the current study.

2.1.1. *Microstructural characterization*

Field emission gun scanning electron microscopy (FEG-SEM, MIRA3-TESCAN, Brno-Kohoutovice, Czech Republic) was performed to visualize the surface and microstructure characteristics of the FRC. Energy dispersive spectroscopy (EDS) was conducted to analyze the elemental and chemical composition of the FRC (INCA Energy EDS System, Oxford Instruments, Concord, MA, USA; incorporated into a TM-3000 Hitachi microscope, Hitachi, Schaumburg, IL, USA).

Please cite this article in press as: Bergamo ETP, et al. Physicochemical and mechanical characterization of a fiber-reinforced composite used as frameworks of implant-supported prostheses. Dent Mater (2021), https://doi.org/10.1016/j.dental.2021.03.014

2.1.2. Crystallinity

The crystallinity of the FRC was analyzed by X-ray diffraction (XRD, X'Pert Powder diffractometer, PANalytical Products, Cambridge, United Kingdom). The scanning was performed on the Bragg θ-2θ geometry, equipped with a graphite monochromator and Cu Kα radiation (λ = 1.5406 Å), operating at a voltage of 40 kV and a current emission of 40 mA. The data were obtained over 2θ range of 10–90° at scan rate of 0.2°/min and step size of 0.020°.

2.1.3. Molecular component analysis

Fourier transform infrared spectrometer (FTIR) spectra of the FRC were recorded on Frontier spectrometer (PerkinElmer Inc., Waltham, MA, USA) equipped with a universal attenuated total reflection (UATR) accessory. Each spectrum was acquired in transmittance mode by accumulation of 16 scans with a range of 4000−500 cm^{-1}.

2.1.4. Thermal degradation behavior

The simultaneous thermogravimetric analysis with differential scanning calorimetry (DSC/TGA, STA 449 F3 Jupiter, NETZSCH-Gerätebau GmbH, Selb, Germany) of the FRC was carried out from 30 °C to 900 °C with a heating rate of 10 °C/min under a nitrogen atmosphere.

2.1.5. Microhardness

The surface microhardness was measured based on the mean value of three Vickers impressions performed on the surface of 10 samples, with a load of 1 kgf and dwell time of 15 s (Microhardness tester HMV-2000, Shimazu Scientific Instruments, Tokyo, Japan). After measuring the impressed diagonals, the Vickers microhardness values were calculated by: HV = 1.850L (/(d1 × d2)), where L is the load (kgf) and d is the arithmetic mean of the length of the two diagonals (mm).

2.2. Reliability and failure mode

2.2.1. Sample preparation

Eighty-four (4.1 × 10 mm) stainless steel hexagonal implant analogs (Intra-Lock, Intra-Lock, Boca Raton, FL, USA) and prefabricated titanium abutments (PCCH Intra-Lock, Intra-Lock) were used in the present study. Two implants per fixed dental prosthesis (FDP) were embedded with the aid of a surveyor (B2, Bio-Art, Sao Carlos, SP, Brazil) in poly(methylmethacrylate) acrylic resin (Classical, Campo Limpo Paulista, SP, Brazil) leaving 1 mm of the implant-abutment interface exposed and an inter-implant distance of 19 mm, which represented the dimensions to reconstruct a mandibular first molar pontic. The respective abutments were torqued to the implants (30 N cm) using an electronic torque wrench (Tohnichi BTG150CN-S, Tohnichi America, Buffalo Grove, IL, USA). The assembly was scanned and the model of a FDP including second premolar, first molar and second molar was virtually designed with the same anatomy of previously FDPs tested in our laboratory to allow comparison between FRC to metal and zirconia frameworks [15,27]. Through the created model, FRC infrastructures were milled with a conventional (9 mm^2 in the connector area) and modified design (lingual collar height of 2.5 mm height at the cervical region of the framework, connected to proximal struts of 3 mm height resulting in a 12 mm^2 connector area). A hybrid resin composite system with approximately 73% zirconium silicate inorganic compound (Ceramage, Shofu, Kyoto, Japan) was used to restore the final teeth anatomy of the FDPs (approximately 1 mm thickness). FRC frameworks were sandblasted with alumina particles of 45 μm for 10 s at a distance of 5 mm, washed and rinsed, and air dried. For adhesive bonding, a layer of primer followed by application of the bond system (CeraResin Bond, Shofu) were applied on the framework surface with a microbrush, thus light-cured for 20 s each surface (Valo Corded, Ultradent Products, South Jordan, UT, USA). The veneering composite reconstruction was performed with the incremental technique using a prefabricated silicone matrix obtained from the printed model of the FDP anatomy to standardize final prostheses geometry.

Subsequently, FDPs were cemented on the abutments using a dual-curing self-adhesive resin cement (BeautiCem SA, Shofu). The intaglio surface of the FRC abutments was sandblasted following the above-mentioned protocol. The samples were washed and rinsed and dried with compressed air. For bonding, the resin cement was directly applied on the internal surface of the FDP using the cement automix dispenser. After setting, the assembly was maintained under a load of 10 N to allow uniform cement spreading and the excess was removed. The FDP margins were light-cured for 20 s on each surface. The samples were stored in deionized water for 48 h prior to mechanical testing [15,27].

2.2.2. Step-stress accelerated life testing (SSALT)

Three FDPs of each group, conventional and modified framework design, underwent single load to failure (SLF) testing using an all-electric dynamic test instrument (ElectroPuls™ E3000 Linear-Torsion system, Instron, Norwood, MA, USA) equipped with a 6.25 mm diameter spherical tungsten carbide indenter positioned at the center of the pontic and a 5000 N load cell at cross-head speed of 1 mm/min.

Mean load-to-failure values were used to delineate three stress profiles for SSALT: mild (n = 9), moderate (n = 6), and aggressive (n = 3), with the distribution of the specimens of each group at a ratio of 3:2:1, respectively (n = 18/group) [28]. These profiles are named based on the step-wise load increase that the specimen will be fatigued throughout the cycles until a certain level of load, meaning that specimens assigned to a mild profile will be cycled longer to reach the same load level of a specimen assigned to the aggressive profile. SSALT was performed using the same all-electric dynamic test equipment with samples immersed in water at a frequency of 10 Hz. The load was also applied at the occlusal surface of the pontic using the same spherical indenter. The test was conducted until specimen failure or suspension (absence of fracture until the end of the determined profile). Fatigue loads throughout SSALT ranged from 200 N up to a maximum of 2000 N with a steady increase in load as a function of elapsed cycles and the findings were recorded as fracture load, stress profile and number of cycles in which the sample failed.

Data analysis consisted of an underlying life distribution to describe the life data collected at different stress levels and a life-stress relationship to quantify the manner in which the life distribution changed across different stress levels [28–31]. Thus, the Weibull Distribution was chosen to fit the life data collected in SSALT and its probability density func-

Please cite this article in press as: Bergamo ETP, et al. Physicochemical and mechanical characterization of a fiber-reinforced composite used as frameworks of implant-supported prostheses. Dent Mater (2021), https://doi.org/10.1016/j.dental.2021.03.014

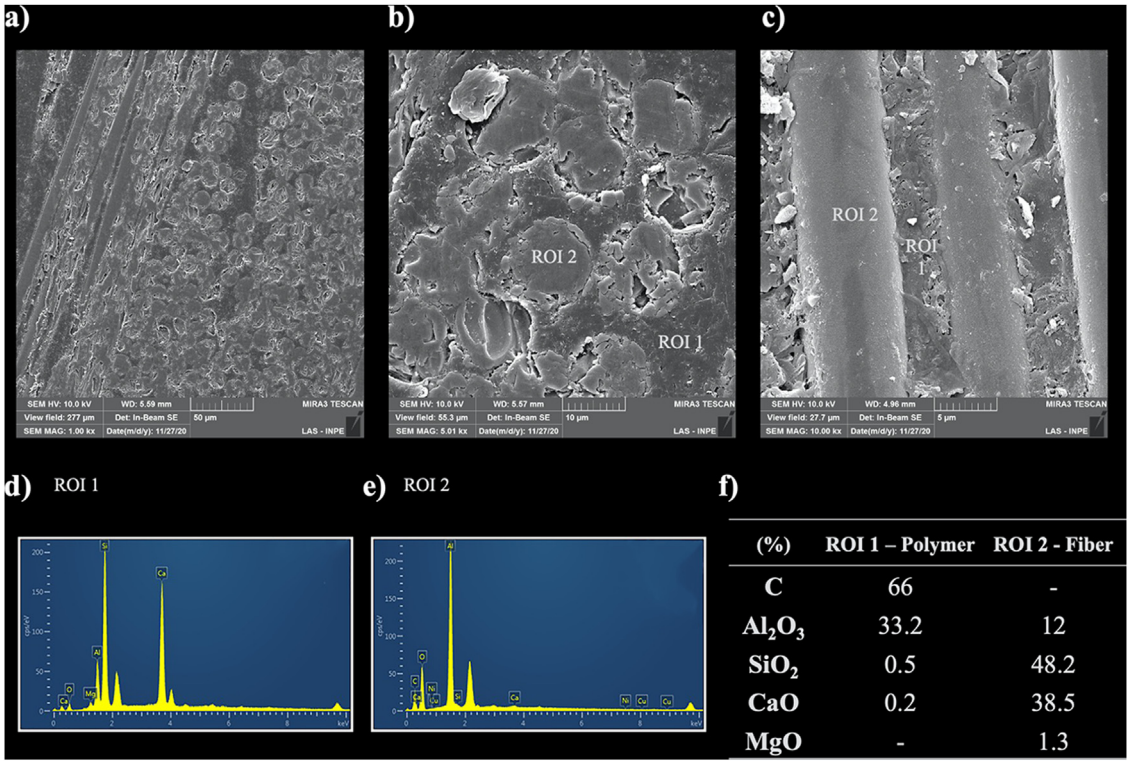

Fig. 1 – Cross-sectional FEG-SEM micrographs of the RFC system (a–c). Chemical composition obtained by energy dispersive spectroscopy in two different regions of interest (ROI), either predominantly polymer (ROI 1) or fiber (ROI 2) (d–f).

tions (pdfs) would be given by: $\int(T) = \frac{\beta}{\eta}\left(\frac{T}{\eta}\right)^{\beta-1} e^{\left(\frac{T}{\eta}\right)^{\beta}}$, where η = scale parameter, and β = shape parameter. Considering the time-varying stress model (x(t)), the inverse power law relationship (IPL) was selected to extrapolate a use level condition considering the cumulative effect of the applied stresses, commonly referred as the cumulative damage model. In such a model, the IPL would be given by $L(x(t)) = (\alpha/x(t))^{\eta}$, where L = life data, and x(t)=stress. Then, the IPL-Weibull pdf (where η is replaced by the IPL) was given by: $\int(t, x(t)) = \beta\left(\frac{x(t)}{\alpha}\right)^{n}\left(\int_0^t\left(\frac{x(t)}{\alpha}\right)^{n}du\right)^{\beta-1} e^{-\left(\left(\frac{x(t)}{\alpha}\right)^{n}du\right)^{\beta}}$. From the extrapolated use level pdf, a variety of functions was derived, including reliability $R(t, x(t)) = e^{-\left(\left(\frac{x(t)}{\alpha}\right)^{n}du\right)^{\beta}}$. Parameters estimation for all analyses was accomplished via MLE method, and 90% two-sided confidence interval (90%CI) was approximated using the Fisher matrix approach. Hence, the use level probability Weibull curves (probability of failure versus number of cycles) with a set load of 300 N were calculated and plotted (Synthesis 9, Alta Pro, Reliasoft, Tucson, AZ, USA). The reliability was calculated for completion of a mission of 100,000 cycles at 300, 600, and 800 N and the differences between groups were identified based on the non-overlap of the CI. As the calculated use level probability Weibull beta parameter of the modified framework group was <1, a Weibull 2-parameter calculation of the Weibull modulus, a unitless parameter that measures the variability of the results, and the characteristic strength, load at which 63.2% of the specimens would fail, was presented using the final load failure or survival (Weibull 9++, Reliasoft) [28,30,31]. Weibull 2-parameter contour plot (Weibull modulus versus characteristic strength) was graphed to determine statistical differences through the non-overlap of CI.

2.2.3. *Fractographic analysis*

Failed FDPs were first inspected in polarized light stereomicroscope (AxioZoom V16, Zeiss, Oberkochen, Germany) using Z-stack mode which automates sequential imaging along the z-plane and sticks them within the same depth of focus (ZEN 2.3 PRO, Zeiss) to depict fracture planes and allow fractographic analysis under higher magnifications (up to 260×). Subsequently, representative samples were evaluated in scanning electron microscope (JEOL T220A, JEOL, Tokyo, Japan) to map the origin and direction of crack propagation. Criteria used for failure were fixation screw fracture and/or abutment fracture, veneering material chipping (cohesive), veneering material fracture exposing the FRC framework (adhesive), and/or infrastructure fracture (catastrophic).

3. Results

The FRC cross-section micrographs obtained by FEG-SEM demonstrated a high density of continuous fibers in intimate contact with the polymer matrix, as well as their standardized cylinder geometry (15 μm diameter) and parallel distribution in a multi-layer bidirectional fashion (Fig. 1a–c). Chemical composition was obtained by energy dispersive spectroscopy

Please cite this article in press as: Bergamo ETP, et al. Physicochemical and mechanical characterization of a fiber-reinforced composite used as frameworks of implant-supported prostheses. Dent Mater (2021), https://doi.org/10.1016/j.dental.2021.03.014

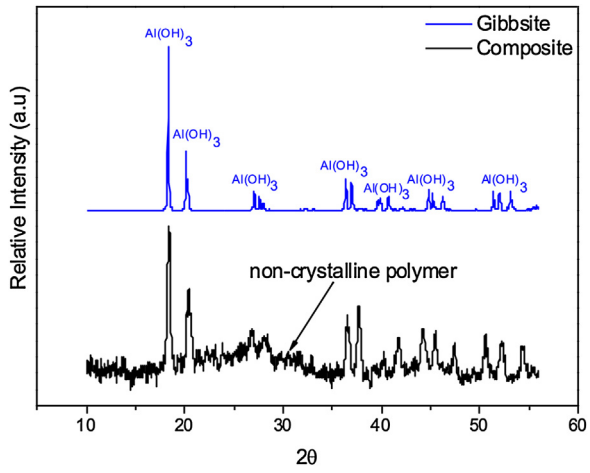

Fig. 2 – X-ray diffraction spectra of the FRC, where the crystalline content consisted of gibbsite, which is a crystalline phase of aluminum hydroxide, $AL(OH)_3$.

(EDS) in two different regions of interest (ROI), either predominantly polymer or fiber. While the polymer ROI was composed of approximately 66% carbon and 33% aluminum oxide, fiber ROI consisted of approximately 48% silicon dioxide and 38% calcium oxide (Fig. 1d-f). X-ray diffraction (XRD) spectra revealed a mostly amorphous material with few peaks typical of aluminum hydroxide ($Al(OH)_3$) (Fig. 2). Based on EDS and XRD spectra, it can be inferred that the FRC analyzed in the current study was reinforced with glass fibers due to the predominant presence of silica and absence of silicate peaks, as well as gibbsite, which is a crystalline phase of aluminum hydroxide.

Fig. 3 shows the Fourier transform infrared spectrometer (FTIR) spectra and band assignments for the FRC. The spectra exhibited similarities in band shape and peak positions with the previously reported for diglycidyl ether of novolac phenol formaldehyde resin [32,33], indicating that this type of epoxy resin was used as the polymer matrix of the FRC. The broad spectroscopic vibration at 3430 cm^{-1} has been associated with stretching of hydroxyl groups (O—H), and bands setting at 1600–1500 cm^{-1} was attributed to the aromatic ring stretching of C=C phenyl groups. The bands in the range of 3067–2850, 1485, and 1345–1230 cm^{-1} correspond to vibrations of aromatic and aliphatic C–H groups, such as CH_2 and CH_3. Epoxy groups vibrations can be observed at 3067–2850, 1230–1345, and 940–972 cm^{-1}. The wavenumber at 3382 and 669 cm^{-1} was attributed to vibrations of amino groups, which may be associated with curing agents.

Thermogravimetric curves analysis demonstrated a minor weight loss at 130 °C, corresponding to the removal of moisture (~1.5% weight loss). Subsequently, a mild weight loss at 300 °C was associated with the dehydration of the aluminum hydroxide (gibbsite $Al(OH)_3$ to boehmite AlOOH) (~5.5% weight loss), and a more intense weight loss starting at 420 °C was attributed to the decomposition of the epoxy resin (~25% weight loss). A last thermal event was observed from 450 to 800 °C, which corresponds to the dehydration of the boehmite (~3% weight loss), forming alumina (Al_2O_3, ~20% weight content) [34]. Based on the percent weight loss of FRC constituents, glass fiber content could be estimated at approximately ~45% (Fig. 4).

Microhardness using Vickers indenter applying a load of 1 kgf for 15 s provided a value of 212 (CI: 14) HV for the investigated FRC.

Use level probability Weibull curves calculated from the step-stress accelerated life testing (SSALT) data for a use level

a)

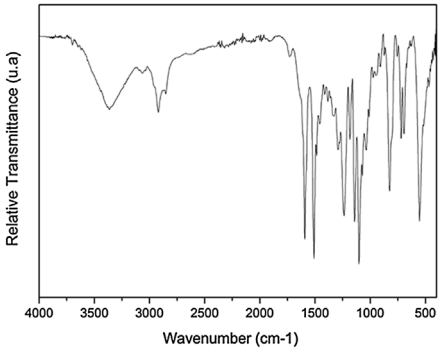

b)

Wavenumber (cm^{-1})	Band assignments
3430	ν OH free
3382	*νs* N–H
3067 2962 2910 2850	Combination bands *ν* COC epoxy, *νs* CH3, *ν* CH *ν* CH aromatic ring, *νa* CH_2, *ν* CH, *νs* CH_3
1600 1500	*ν*C=C aromatic ring
1485	δ CH_2
1345 1230	δ CH3, νC–O, ν COC epoxy
1140 1100	δ Ar–H, ν C–O
1078 1031	δ C–N, ν C–O
972 940	ν COC epoxy
830	δ Ar–H
669	δ NH

Fig. 3 – Fourier transformed infrared spectra of the FRC (a). Bands assignments for the glass fiber-reinforced composite (b), where *ν* = stretching, *νa* = asymmetric stretching, *νs* = symmetric stretching, δ = bending.

Please cite this article in press as: Bergamo ETP, et al. Physicochemical and mechanical characterization of a fiber-reinforced composite used as frameworks of implant-supported prostheses. Dent Mater (2021), https://doi.org/10.1016/j.dental.2021.03.014

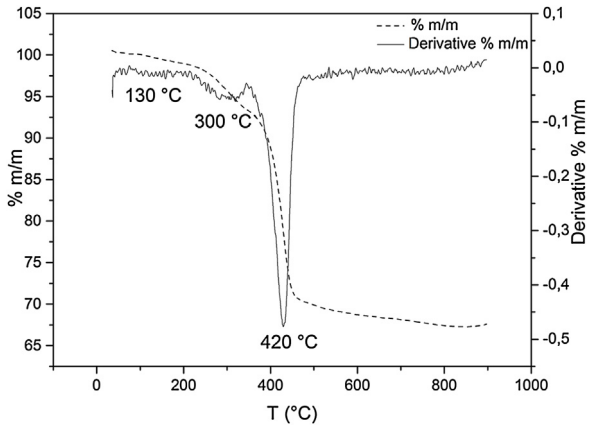

Fig. 4 – Thermogravimetric curve and derivative thermogravimetric curve of the FRC.

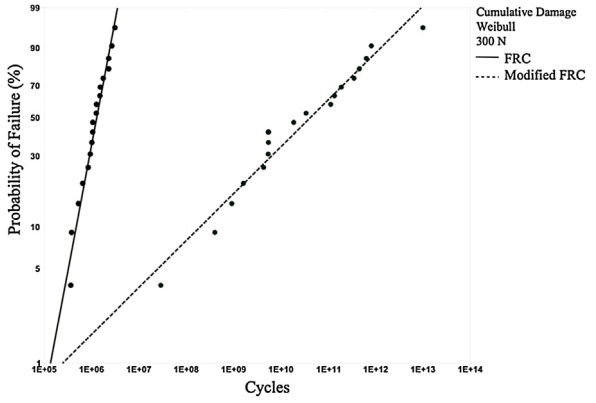

Fig. 5 – Use level probability Weibull curves evidencing the probability of failure as a function of elapsed cycles for FRC fixed partial dentures at a use level load of 300 N.

load of 300 N were plotted in the Fig. 5. The cumulative damage model calculations using a Weibull distribution and an inverse power law life-stress relationship exhibited beta values (β, Weibull configuration factor) of 1.87 (CI: 0.89–3.96) for conventional and 0.35 (CI: 0.06–1.17) for modified FRC FDPs, which indicate that fatigue damage accumulation was the main acceleration factor for failure of the former, whereas failure rates did not increase with fatigue and strength was the main element influencing failure of the latter. It is noteworthy that the lower bound of the CI of conventional FRC FDPs denotes an effect of strength influencing failure rate ($\beta < 1$).

Table 1 shows the reliability calculated for completion of a mission of 100,000 cycles at predetermined loads of 300, 600, and 800 N along with the bilateral 90% confidence intervals (CI) for conventional and modified FRC FDPs. Three-unit implant-supported prostheses with FRC frameworks demonstrated a high probability of survival (up to 99%, CI: 95–100%) for an estimated masticatory load of molar regions, 300 N, irrespective of framework design. Conventional FRC FDPs (84%, CI: 69–92%) demonstrated a statistically significant decrease in the reliability at a set load level of 600 N, whereas modified FRC FDPs data (94%, CI: 77–98%) were not significantly reduced, with both framework designs statistically homogeneous. The

Table 1 – Reliability and the respective 90% bilateral confidence interval of FRC fixed partial dentures for an estimated mission of 100,000 cycles at 300, 600, and 800 N.

	FRC	Modified FRC
Upper Bound	100	100
Reliability at 300 N	**99 aA**	**99 aA**
Lower Bound	97	95
Upper Bound	92	98
Reliability at 600 N	**84 aB**	**94 aAB**
Lower Bound	69	77
Upper Bound	34	91
Reliability at 800 N	**19 bC**	**75 aB**
Lower Bound	8	42

Different lowercase letters indicate statistical difference between framework design. Different uppercase letters indicate statistical difference between missions.

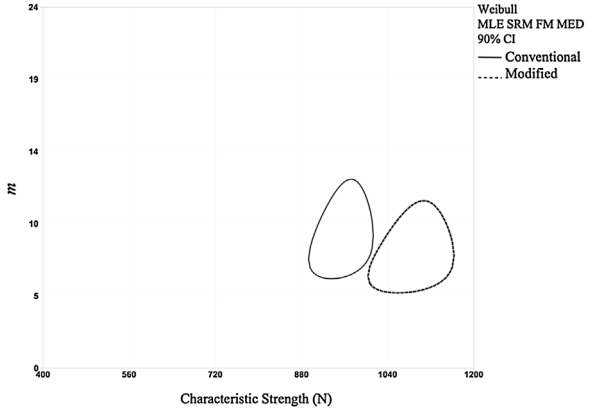

Fig. 6 – Weibull two-parameter contour plot evidencing the characteristic strength (N) and Weibull modulus (m) of the conventional and modified FRC framework designs. The non-overlap of the contours indicates statistically significant difference.

cumulative damage reaching a high-load magnitude, 800 N, also resulted in a statistically significant decrease in the probability of survival for conventional FRC FDPs (19%, CI: 8–34%), and the percentage was significantly lower relative to modified FRC FDPs (75%, CI: 42–91%). Modified FRC FDPs reliability only presented statistically significant difference between 300 and 800 N missions.

Data analyzed as a function of fatigue load at failure using Weibull distribution depicted a Weibull modulus (*m*) of 9.02 (CI: 6.90–11.96) for the conventional and of 7.75 (CI: 5.73–10.50) for modified FRC FDPs. The characteristic strength demonstrated significantly higher values for modified (1,0831083 N, CI: 1,027−1141 N) relative to conventional (941 N, CI: 904−980 N) FRC FDPs. Two-parameter Weibull contour plot showing the non-overlap of the confidence bounds between framework designs is presented in the Fig. 6.

The main failure modes demonstrated by the FRC FDPs were the cohesive fracture of the veneering composite on lower loads (chipping, 650−725 N) as well as, at higher loads, the adhesive fracture of the veneering composite with infrastructure exposure (720−1225 N) (Figs. 7 and 8). FRC FDPs with

Please cite this article in press as: Bergamo ETP, et al. Physicochemical and mechanical characterization of a fiber-reinforced composite used as frameworks of implant-supported prostheses. Dent Mater (2021), https://doi.org/10.1016/j.dental.2021.03.014

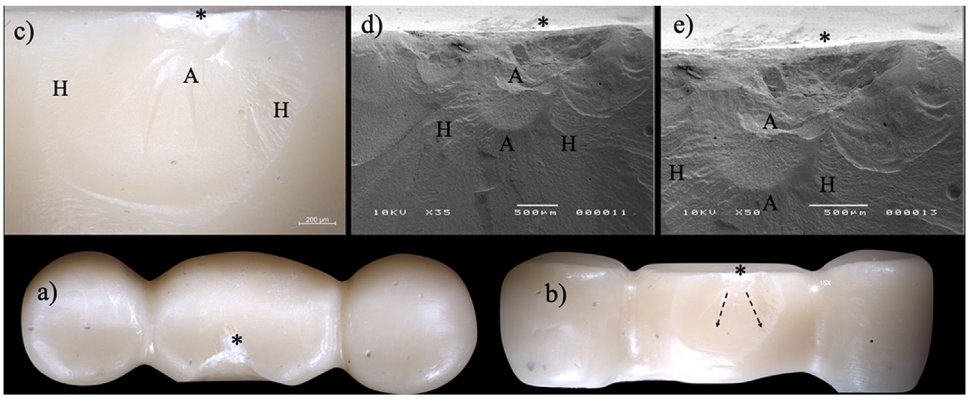

Fig. 7 – Stereomicroscope and SEM images of a representative veneering composite cohesive fracture. The micrographs indicate the origin (*) and the direction of crack propagation (arrows), with crack initiating under the loading surface and propagating all the way through the cervical margin of the FPD. Fractographic marks support the direction of crack propagation by the presence of multiple hackle lines (H) and arrest lines (A).

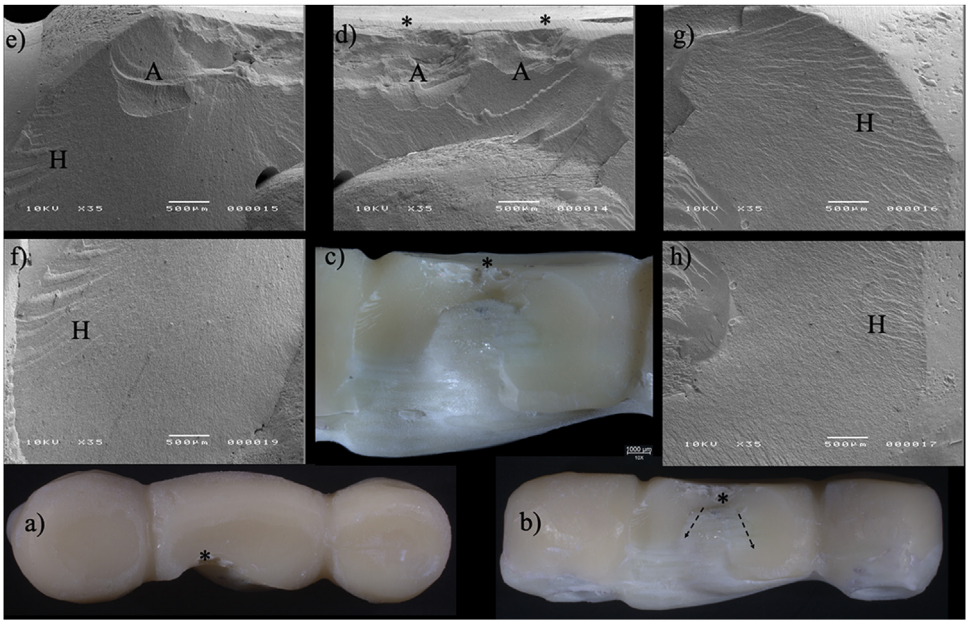

Fig. 8 – Stereomicroscope and SEM images of a representative veneering composite adhesive fracture. The micrographs indicate the origin (*) and the direction of crack propagation, with multiple cracks initiating under the loading surface and propagating all the way through the proximal and cervical margins of the FDP. Fractographic marks support the direction of crack propagation by the presence of multiple hackle lines (H) and arrest lines (A).

conventional framework presented more catastrophic failure with veneering composite and framework fractures (n = 7) relative to modified frameworks (n = 1) (850–1050 N) (Fig. 9). Careful examination of the occlusal surface of FRC FDPs revealed the typical fatigue wear of polymeric materials under the loading area before fracturing. Cohesive fracture of the veneering composite started from the occlusal indentation area, leading to subsurface damage and cone crack propagation towards the cervical margin of the restoration (Fig. 7). Continued damage accumulation and microcracking under the loading area were verified in FRC FDPs with adhesive fracture, where cracks originating from multiple crack fronts propagated as the load and number of cycles increased and resulted in veneering composite delamination (Fig. 7). FRC FDPs framework fracture was associated with competing failure modes, where besides occlusal cracks fronts, an additional crack front originating from the tensile side (gingival) of the connectors toward the occlusal surface resulted in catastrophic failure (Fig. 8). Telltale fractographic marks including hackles and arrest lines confirmed the current findings.

Neither implants nor abutments presented bending or fracture for both framework designs.

4. Discussion

Advantages of FRC CAD/CAM systems may lie on their high strength-to-weight ratio, resistance-curve (R-curve) behavior, and low elastic modulus in tandem with excellent reliabil-

Please cite this article in press as: Bergamo ETP, et al. Physicochemical and mechanical characterization of a fiber-reinforced composite used as frameworks of implant-supported prostheses. Dent Mater (2021), https://doi.org/10.1016/j.dental.2021.03.014

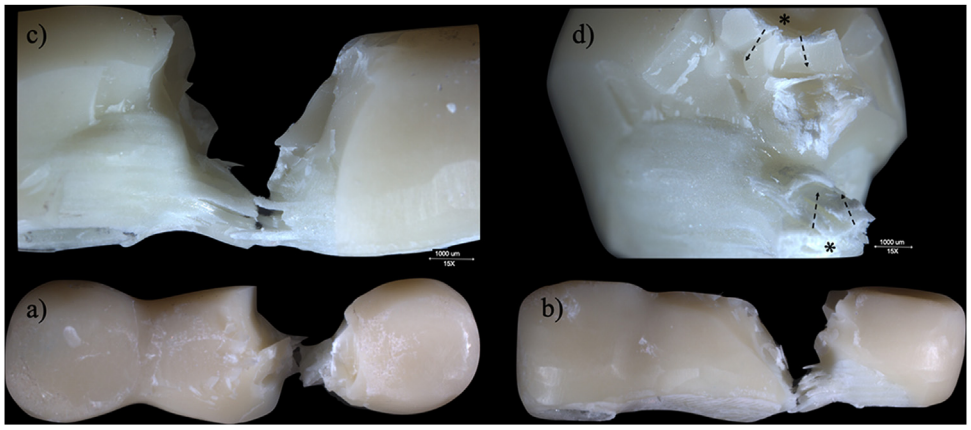

Fig. 9 – Stereomicroscope images of a representative veneering composite and framework fracture. Besides occlusal cracks fronts (*), an additional rupture front propagated from the gingival side (*) of the connectors towards de occlusal surface resulting in catastrophic failure (arrows).

ity and repairability of dental prostheses [13,15,18–21]. The current study aimed to characterize the physicochemical and mechanical properties of a FRC CAD/CAM system for dental application and to evaluate the reliability and failure mode of FDPs with two framework designs for 3-unit posterior implant-supported prostheses subjected to step-stress accelerated-life fatigue testing (SSALT). Based on the characterization results, the investigated CAD/CAM FRC consisted of an epoxy resin matrix with approximately 28% of crystalline inorganic compounds and 45% of continuous regular-geometry glass fibers parallelly distributed in a multi-layer bidirectional manner. FRC FDPs demonstrated high reliability for a masticatory load in the posterior region of the mouth, irrespective of framework design. Nonetheless, in a more demanding loading scenario, frameworks with a modified design resulted in higher reliability than conventionally designed frameworks. This finding is of relevance since most CAD/CAM systems produce the conventional design as default and additional time must be devoted to computer design a modified framework. Despite the higher occurrence of framework fractures for the conventional infrastructure design, cohesive or adhesive fracture of the veneering composite were the main reported events for FRC FDPs failure. Hence, the postulated null hypothesis that framework design would not affect FRC FDP performance was rejected.

The polymer matrix of the FRC is basically composed of a thermoset epoxy resin, which has been of particular interest to dental application due to its superior attributes related to low thermal conductivity, processing versatility along with favorable fracture toughness and mechanical strength, low elastic modulus and hardness (herein calculated at 212 HV) [35,36]. The structure of the phenol-containing molecule and the number of phenol groups per molecule characterize the epoxy resin type and the final properties of the composite [36]. According to the Fourier transform infrared spectroscopy (FTIR), the diglycidyl ether of novolac phenol formaldehyde resin, instead of most common type, diglycidyl ether of bisphenol A, composed the FRC system. The rationale for using such formulation may lie on the increased formation of epoxide groups, favoring the reaction with amino groups and enhancing the conversion of monomers into a three-dimensional cross-linked network [32]. Some degree of cytotoxicity has been associated with the presence of unreacted amino-functional groups [37]. Moreover, energy dispersive spectroscopy (EDS) and X-ray diffraction (XRD) indicated the formation of gibbsite in the FRC matrix, which is a crystalline phase of aluminum hydroxide. The addition of gibbsite has been associate with its beneficial effects on enhancing the mechanical properties of the system, as well as on increasing its thermal stability, which can favor CAD/CAM use by reducing the detrimental effects of the heating associated with milling process on the FRC properties [35].

The fiber reinforcement of the current FRC consisted of continuous regular-diameter fibers parallelly aligned in a multi-layer bidirectional fashion, which has been properly achieved through the conformation of prefabricated FRC discs under an industrial environment, minimizing the formation of defects and improving the mechanical properties of the material [23–25]. The Weibull modulus, a parameter used to describe the variation in strength values and structural reliability as a result of flaw population [28,30,31], has ranged from approximately 6–12 for the FRC FDPs in the current study, which is within the range of values (5–15) obtained for the currently available indirect systems [38]. Moreover, EDS and XRD data revealed that glass fibers were used in the investigated FRC, which has been widely indicated as reinforcing compounds in FRC systems as a result of their excellent thermal and chemical stability, as well as mechanical strength (σ: approximately 400 MPa) and wear resistance [39]. Nonetheless, machining glass FRC can be relatively slow and challenging, reducing tool life while working on conventional systems [39,40]. Different fiber types and machining systems, as lasers, have been developed and require further investigation concerning their physicochemical characterization and machining performance, respectively [40].

The conformation of reliable FRC discs for CAD/CAM use, as the one herein characterized, have broadened their clinical application, including the biomechanically challenging scenario inherent to implant-supported reconstructions [15]. Previous studies have indicated that framework material

Please cite this article in press as: Bergamo ETP, et al. Physicochemical and mechanical characterization of a fiber-reinforced composite used as frameworks of implant-supported prostheses. Dent Mater (2021), https://doi.org/10.1016/j.dental.2021.03.014

and design influenced FDPs performance [5,9,13,15,16,27,41], encouraging the current investigation of SSALT performance of 3-unit posterior FRC FDPs with a conventional (9 mm^2 connector) and modified (12 mm^2 connector and 2.5-mm height lingual extension) framework designs. FRC FDPs demonstrated high probability of survival at a masticatory load (300 N, 99%) [42], irrespective of framework design. However, modified FRC FDPs (800 N, 75%) resulted in significantly higher reliability relative to the conventional FRC FDPs (800 N, 19%) at a high-load mission. Similarly, Weibull analysis considering the fatigue load at failure showed significantly higher values for modified relative to conventional framework FRC FDPs. SSALT data obtained under a similar protocol for FDPs of a different CAD/CAM FRC system with different framework designs, 9 mm^2 and 12 mm^2 connector, have demonstrated higher reliability for the 12 mm^2 connector at 300 N (79% and 96%, respectively), which was similar to the results obtained for both frameworks tested in the current study [15]. Moreover, porcelain-veneered MC and Y-TZP FDPs with 12 mm^2 of connector have also been tested under the same protocol, with reliability estimated at a similar percentage for MC FDPs (300 N, 95%) and at a significantly lower percentage for Y-TZP FDPs (300 N, 55%) relative to the current FRC FDPs [27]. The comparison with the available indirect systems indicates a promising outcome for the newly developed FRC under a challenging clinical scenario. Moreover, the results corroborate with the principle that other properties besides mechanical strength may contribute to rehabilitations survival, especially in implant-supported reconstructions that seem to be more prone to technical complications due to the absence of periodontal ligament and critical biomechanical behavior [5,8,9,15,16,24]. The favorable performance of FRC FDPs can be associated with their low elastic modulus and flexible nature, making them more suitable for loading energy absorption and stress distribution [15,16]. Resilient restorative systems may also account for reduced stress transmission to peri-implant bone and, consequently, reduced long-term biological complications [8,9,16].

The failure of all tested FRC FDPs occurred at loads above the average maximum bite forces at the molar region [42]. Despite the aforementioned results, the weakest link of FRC FDPs still comprised the veneering material by cohesive (at lower loads) or adhesive (at higher loads) fracture of the veneering composite where cracks originated under the loading area propagated to the margins of the prostheses [15,43]. The favorable load-at-failure has been associated with the physical-mechanical properties of the CAD/CAM FRC, the bidirectional alignment of the multi-layer continuous glass fibers along with the anatomic design of the frameworks [13,15,16,44]. Biomechanically, continuous fibers should be parallelly aligned with the maximum principal stress direction to deliver the maximum effectiveness of the rehabilitation [13–17,44]. However, previous studies have reported that the most common failure mode of hand made FRC prostheses with unidirectional fiber alignment was indeed the veneering composite fracture as a result of framework insufficient occlusal support, thus bidirectional fibers have been suggested to increase prosthesis fracture resistance [13,18,44]. Based on such premise, the high load-at-failure of the FRC FDPs may also be related to the multi-layer bidirectional fiber alignment that have provided an additional reinforcement effect in different stress direction for the veneering composite [44]. The occurrence of cohesive or adhesive veneering composite fracture may be associated with the relative position of the fiber content within the framework of the specific loaded area, affecting damage initiation and propagation [45], as well as defects from the compromised interfacial adhesion of the epoxy/methacrylate interface [46,47]. In addition, the modified framework design has also promoted higher resistance against catastrophic failure, with only 1 framework fracture relative to 7 observed in the conventional framework group, which may be the result of increased flexing of the latter during testing [13,15]. The modified framework design may have provided an increased support due to the higher cross-sectional fiber content, contributing to the highest load-bearing capacity [44,45,48].

An important advantage regarding the predominant failure modes of the FRC FDPs, which was cohesive within the veneering composite, is the possibility of clinical repair through conventional in-office restorative procedures [14,15,49]. Moreover, in bonding veneering composites to FRCs, the exposed fibers and the polymer matrix are the substrates for adhesion [47]. Hence, it is important to mention that the adhesive failures may be related to a compromised bond strength of the epoxy/methacrylic interface, as well as a consequence of the three-dimensional fiber position [46,50]. First, the exposed glass fibers (approximately 45% volume content of the FRC) have to be silanized to improve bond strength to the veneering composite at the interface [47], as performed in the current study. Second, when the orientation of the exposed fibers is considered, the highest bond strength to the FRC surface would be obtained with perpendicularly exposed fibers at the interface [50], however, such an arrangement does not favor the mechanical strength of the framework, where fiber alignment should be perpendicular to the maximum principal stress direction [13–17,44]. Despite the unfavorable fiber position for adhesive purposes, previous studies have indicated that bonding efficiency of FRCs with different orientations of fibers varies only slightly from each other, especially for the vertically exposed fibers relative to the perpendicular ones [50–52]. Considering the polymer matrix, the FRC is composed of epoxy resin (approximately 25% volume content of the FRC) and the veneering composite of methacrylate-based resin, whose solubility is not favorable [46]. Usually, adhesion mechanisms of indirectly fabricated composites are based on the dissolution of the surface and polymer chain entanglement between the dissolved substrate and monomers of the veneering material (the so-called semi-IPN bonding formation); however, thermoset cross-linked polymers, such as the current FRC system, are difficult to dissolve without strong chemicals, high pressure or temperature, therefore bonding must be carefully addressed [47,53]. Another concern of the current scenario is the absence of the non-polymerized surface layer due to presence of air, common to direct FRC reconstructions, which would favor by free radical polymerization the formation of a stable chemical bond [47]. Based on such concerns and to obtain a favorable adhesion of the veneering composite to the FRC, micromechanical retentions using surface blasting methods should be performed [54], protocol adopted in the present study. Such aspects can be

Please cite this article in press as: Bergamo ETP, et al. Physicochemical and mechanical characterization of a fiber-reinforced composite used as frameworks of implant-supported prostheses. Dent Mater (2021), https://doi.org/10.1016/j.dental.2021.03.014

considered as limitations of the current FRC system and support further investigations concerning the use of different physicomechanical surface pretreatments, including different protocols of surface blasting (i.e. silica coating) and/or the development of tailored adhesive/primer systems, to improve interfacial bond strength [13–17,44,46]. A potential mechanism to obtain monomer diffusion into the surface layer of the cross-linked FRC composite may be based on the use of a transesterification reaction, though it requires relative high temperatures, approximately 180 °C, which may affect clinical use [53]. Also, the aforementioned facts encourage future investigations concerning the performance of indirect systems cemented on FRC frameworks, such as CAD/CAM composites or glass ceramics, which has already demonstrated higher reliability and mechanical strength relative to their direct counterparts to improve the load bearing capacity of the reconstructions, though they probably would not change the predominant failure mode [26,55]. However, whether increased bond strength between resin composite and FRC framework, as well as increased mechanical properties of veneered material would synergistically translate to higher success rates are yet to be confirmed in clinical studies."

5. Conclusion

The CAD/CAM composite system evaluated in the current study consisted of regular-geometry glass fibers parallelly distributed in a multi-layer bidirectional fashion into an epoxy resin matrix, with inorganic compounds and fiber content of approximately 75%. Fixed dental prostheses fabricated with the fiber-reinforced composite demonstrated high reliability in a mission that corresponds to physiological masticatory load in the molar region, irrespective of framework design. Nonetheless, in a challenging functional scenario, >600 N, lingually extended frameworks resulted in higher reliability relative to conventional frameworks. Despite the higher incidence of framework fractures in the conventional design, the weakest link of the system was the veneering material, with predominant cohesive or adhesive fracture of the veneering composite, which demands improvements and future investigations.

Acknowledgements

To Fundação de Amparo a Pesquisa do Estado de São Paulo (FAPESP) Young Investigators Award grant 2012/19078-7, EMU 2016/18818-8, FAPESP 2019/06893-1, 2019/14798-0, 2018/03072-6/BEPE 2019/00452-5, to Conselho Nacional de Desenvolvimento Científico e Tecnológico (CNPq) grants 304589/2017-9 and 434487/2018-0, and to CAPES Finance Code 001.

REFERENCES

[1] von Stein-Lausnitz M, Nickenig HJ, Wolfart S, Neumann K, von Stein-Lausnitz A, Spies BC, et al. Survival rates and complication behaviour of tooth implant-supported, fixed dental prostheses: a systematic review and meta-analysis. J Dent 2019;88:103167.

[2] Moraschini V, Poubel LA, Ferreira VF, Barboza Edos S. Evaluation of survival and success rates of dental implants reported in longitudinal studies with a follow-up period of at least 10 years: a systematic review. Int J Oral Maxillofac Surg 2015;44:377–88.

[3] Coelho PG, Jimbo R, Tovar N, Bonfante EA. Osseointegration: hierarchical designing encompassing the macrometer, micrometer, and nanometer length scales. Dent Mater 2015;31:37–52.

[4] Sanz-Sanchez I, Sanz-Martin I, Figuero E, Sanz M. Clinical efficacy of immediate implant loading protocols compared to conventional loading depending on the type of the restoration: a systematic review. Clin Oral Implants Res 2015;26:964–82.

[5] Pieralli S, Kohal RJ, Rabel K, von Stein-Lausnitz M, Vach K, Spies BC. Clinical outcomes of partial and full-arch all-ceramic implant-supported fixed dental prostheses. A systematic review and meta-analysis. Clin Oral Implants Res 2018;29(Suppl 18):224–36.

[6] Rabel K, Spies BC, Pieralli S, Vach K, Kohal RJ. The clinical performance of all-ceramic implant-supported single crowns: a systematic review and meta-analysis. Clin Oral Implants Res 2018;29(Suppl 18):196–223.

[7] Pjetursson BE, Bragger U, Lang NP, Zwahlen M. Comparison of survival and complication rates of tooth-supported fixed dental prostheses (FDPs) and implant-supported FDPs and single crowns (SCs). Clin Oral Implants Res 2007;18(Suppl 3):97–113.

[8] Conserva E, Menini M, Tealdo T, Bevilacqua M, Ravera G, Pera F, et al. The use of a masticatory robot to analyze the shock absorption capacity of different restorative materials for prosthetic implants: a preliminary report. Int J Prosthodont 2009;22:53–5.

[9] Menini M, Conserva E, Tealdo T, Bevilacqua M, Pera F, Signori A, et al. Shock absorption capacity of restorative materials for dental implant prostheses: an in vitro study. Int J Prosthodont 2013;26:549–56.

[10] Meyer G, Fanghanel J, Proff P. Morphofunctional aspects of dental implants. Ann Anat 2012;194:190–4.

[11] Miyazaki T, Hotta Y, Kunii J, Kuriyama S, Tamaki Y. A review of dental CAD/CAM: current status and future perspectives from 20 years of experience. Dent Mater J 2009;28:44–56.

[12] Silva NR, Witek L, Coelho PG, Thompson VP, Rekow ED, Smay J. Additive CAD/CAM process for dental prostheses. J Prosthodont 2011;20:93–6.

[13] Perea-Lowery L, Vallittu PK. Framework design and pontics of fiber-reinforced composite fixed dental prostheses — an overview. J Prosthodont Res 2018;62:281–6.

[14] Vallittu PK, Shinya A, Baraba A, Kerr I, Keulemans F, Kreulen C, et al. Fiber-reinforced composites in fixed prosthodontics—Quo vadis? Dent Mater 2017;33:877–9.

[15] Bonfante EA, Suzuki M, Carvalho RM, Hirata R, Lubelski W, Bonfante G, et al. Digitally produced fiber-reinforced composite substructures for three-unit implant-supported fixed dental prostheses. Int J Oral Maxillofac Implants 2015;30:321–9.

[16] Erkmen E, Meric G, Kurt A, Tunc Y, Eser A. Biomechanical comparison of implant retained fixed partial dentures with fiber reinforced composite versus conventional metal frameworks: a 3D FEA study. J Mech Behav Biomed Mater 2011;4:107–16.

[17] Gloria A, Ronca D, Russo T, D'Amora U, Chierchia M, De Santis R, et al. Technical features and criteria in designing fiber-reinforced composite materials: from the aerospace and aeronautical field to biomedical applications. J Appl Biomater Biomech 2011;9:151–63.

Please cite this article in press as: Bergamo ETP, et al. Physicochemical and mechanical characterization of a fiber-reinforced composite used as frameworks of implant-supported prostheses. Dent Mater (2021), https://doi.org/10.1016/j.dental.2021.03.014

[18] Ahmed KE, Li KY, Murray CA. Longevity of fiber-reinforced composite fixed partial dentures (FRC FPD)—systematic review. J Dent 2017;61:1–11.
[19] Tiu J, Belli R, Lohbauer U. R-curve behavior of a short-fiber reinforced resin composite after water storage. J Mech Behav Biomed Mater 2020;104:103674.
[20] Freilich MA, Meiers JC. Fiber-reinforced composite prostheses. Dent Clin North Am 2004;48, viii–ix, 545–562.
[21] Bonfante EA, Suzuki M, Hirata R, Bonfante G, Fardin VP, Coelho PG. Resin composite repair for implant-supported crowns. J Biomed Mater Res B Appl Biomater 2016.
[22] Mehdikhani M, Gorbatikh L, Verpoest I, Lomov SV. Voids in fiber-reinforced polymer composites: a review on their formation, characteristics, and effects on mechanical performance. J Compos Mater 2019;53:1579–669.
[23] Muhlemann S, Benic GI, Fehmer V, Hammerle CHF, Sailer I. Clinical quality and efficiency of monolithic glass ceramic crowns in the posterior area: digital compared with conventional workflows. Int J Comput Dent 2018;21:215–23.
[24] Rekow D, Thompson VP. Engineering long term clinical success of advanced ceramic prostheses. J Mater Sci Mater Med 2007;18:47–56.
[25] Sailer I, Benic GI, Fehmer V, Hammerle CHF, Muhlemann S. Randomized controlled within-subject evaluation of digital and conventional workflows for the fabrication of lithium disilicate single crowns. Part II: CAD-CAM versus conventional laboratory procedures. J Prosthet Dent 2017;118:43–8.
[26] Goncu Basaran E, Ayna E, Vallittu PK, Lassila LV. Load-bearing capacity of handmade and computer-aided design–computer-aided manufacturing-fabricated three-unit fixed dental prostheses of particulate filler composite. Acta Odontol Scand 2011;69:144–50.
[27] Bonfante EA, Coelho PG, Navarro Jr JM, Pegoraro LF, Bonfante G, Thompson VP, et al. Reliability and failure modes of implant-supported Y-TZP and MCR three-unit bridges. Clin Implant Dent Relat Res 2010;12:235–43.
[28] Bonfante EA, Coelho PG. A critical perspective on mechanical testing of implants and prostheses. Adv Dent Res 2016;28:18–27.
[29] Bergamo ETP, Bordin D, Ramalho IS, Lopes ACO, Gomes RS, Kaizer M, et al. Zirconia-reinforced lithium silicate crowns: effect of thickness on survival and failure mode. Dent Mater 2019;35:1007–16.
[30] Nelson W. Accelerated testing: statistical models, test plans and data analysis. John Wiley & Sons; 2004.
[31] Zhao WE, EA. A general accelerated life model for step-stress testing. IIE Trans 2005;37:1059–69.
[32] Sales R, Diniz MF, Thim G. Study of curing process of glass fiber and epoxy resin composite by FT-NIR, photoacoustic spectroscopy and luminescence spectroscopy. J Mater Sci 2011;46:1814–23.
[33] Cividanes LS, Simonetti EAN, Campos TMB, Bettoni TS, Brunelli DD, Thim GP. Anomalous behavior of thermal stability of amino-carbon nanotube–epoxy nanocomposite. J Compos Mater 2015;49:3067–73.
[34] Rivas Mercury JM, Sucupira JRM, Rodríguez MA, Cabral AA, de Aza AH, Pena P. Influence of the milling conditions on the thermal decomposition of Bayer gibbsite. Powder Technol 2020;362:188–96.
[35] Patil R, Kankuppi S. Comparison between experimental and theoretical thermal conductivity on epoxy based aluminium hydroxide and silica aerogel composite materials. Mater Today Proc 2019;27(1):509–14.
[36] Atif R, Shyha I, Inam F. Mechanical, thermal, and electrical properties of graphene-epoxy nanocomposites—a review. Polymers 2016;8:1–30.
[37] Yano E. Increased activity of monoamine oxidase by epoxy resin hardeners. Toxicol Lett 1987;37:27–32.
[38] Tinschert J, Zwez D, Marx R, Anusavice KJ. Structural reliability of alumina-, feldspar-, leucite-, mica- and zirconia-based ceramics. J Dent 2000;28:529–35.
[39] Rajak DK, Pagar DD, Menezes PL, Linul E. Fiber-reinforced polymer composites: manufacturing, properties, and applications. Polymers 2019;11:1667.
[40] Prakash S. Experimental investigation of surface defects in low-power CO_2 laser engraving of glass fiber-reinforced polymer composite. Polym Compos 2019;40.
[41] Pjetursson BE, Valente NA, Strasding M, Zwahlen M, Liu S, Sailer I. A systematic review of the survival and complication rates of zirconia-ceramic and metal-ceramic single crowns. Clin Oral Implants Res 2018;29(Suppl 16):199–214.
[42] van der Bilt A, Tekamp A, van der Glas H, Abbink J. Bite force and electromyograpy during maximum unilateral and bilateral clenching. Eur J Oral Sci 2008;116:217–22.
[43] Wendler M, Kaizer MR, Belli R, Lohbauer U, Zhang Y. Sliding contact wear and subsurface damage of CAD/CAM materials against zirconia. Dent Mater 2020;36:387–401.
[44] Xie Q, Lassila LV, Vallittu PK. Comparison of load-bearing capacity of direct resin-bonded fiber-reinforced composite FPDs with four framework designs. J Dent 2007;35:578–82.
[45] Dyer S, Lassila L, Vallittu P. The effect of internal fiber arrangement on the delamination failure in hybrid composite dental prostheses. Физическая мезомеханика 2004;7.
[46] Alnaqbi IOM, Elbishari H, Elsubeihi ES. Effect of fiber post-resin matrix composition on bond strength of post-cement interface. Int J Dent 2018;2018:4751627.
[47] Vallittu PK. Interpenetrating polymer networks (IPNs) in dental polymers and composites. J Adhes Sci Technol 2009;23:961–72.
[48] Dyer SR, Sorensen JA, Lassila LV, Vallittu PK. Damage mechanics and load failure of fiber-reinforced composite fixed partial dentures. Dent Mater 2005;21:1104–10.
[49] Rosentritt M, Behr M, Leibrock A, Handel G, Friedl KH. Intraoral repair of fiber-reinforced composite fixed partial dentures. J Prosthet Dent 1998;79:393–8.
[50] Vallittu PK. High-aspect ratio fillers: fiber-reinforced composites and their anisotropic properties. Dent Mater 2015;31:1–7.
[51] Tezvergil A, Lassila LV, Vallittu PK. The shear bond strength of bidirectional and random-oriented fibre-reinforced composite to tooth structure. J Dent 2005;33:509–16.
[52] Tezvergil A, Lassila LV, Vallittu PK. Strength of adhesive-bonded fiber-reinforced composites to enamel and dentin substrates. J Adhes Dent 2003;5:301–11.
[53] Basavarajappa S, Perea-Lowery L, Alshehri AM, Al-Kheraif AAA, Matinlinna JP, Vallittu PK. Surface dissolution and transesterification of thermoset dimethacrylate polymer by dimethacrylate adhesive resin and organic catalyst-alcohol solution. Dent Mater 2020;36:698–709.
[54] de Oliveira Lino LF, Machado CM, de Paula VG, Vidotti HA, Coelho PG, Benalcazar Jalkh EB, et al. Effect of aging and testing method on bond strength of CAD/CAM fiber-reinforced composite to dentin. Dent Mater 2018;34:1690–701.
[55] Ruse ND, Sadoun MJ. Resin-composite blocks for dental CAD/CAM applications. J Dent Res 2014;93:1232–4.

Please cite this article in press as: Bergamo ETP, et al. Physicochemical and mechanical characterization of a fiber-reinforced composite used as frameworks of implant-supported prostheses. Dent Mater (2021), https://doi.org/10.1016/j.dental.2021.03.014